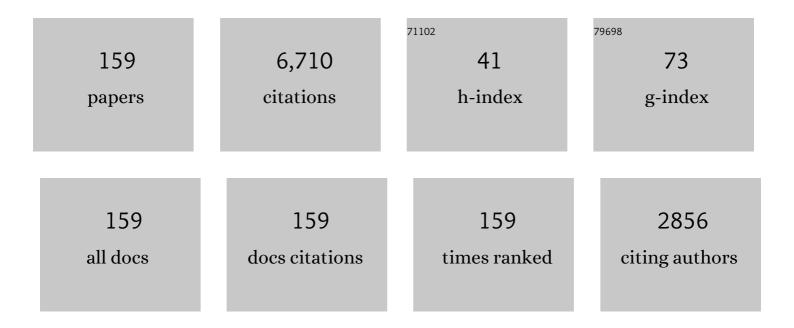
Laurent Pueyo

List of Publications by Year in descending order

Source: https://exaly.com/author-pdf/9009105/publications.pdf Version: 2024-02-01



#	Article	IF	CITATIONS
1	DETECTION AND CHARACTERIZATION OF EXOPLANETS AND DISKS USING PROJECTIONS ON KARHUNEN-LOÃ VE EIGENIMAGES. Astrophysical Journal Letters, 2012, 755, L28.	8.3	571
2	First light of the Gemini Planet Imager. Proceedings of the National Academy of Sciences of the United States of America, 2014, 111, 12661-12666.	7.1	472
3	BANYAN. XI. The BANYAN Σ Multivariate Bayesian Algorithm to Identify Members of Young Associations with 150 pc. Astrophysical Journal, 2018, 856, 23.	4.5	374
4	The Gemini Planet Imager Exoplanet Survey: Giant Planet and Brown Dwarf Demographics from 10 to 100 au. Astronomical Journal, 2019, 158, 13.	4.7	270
5	A New High Contrast Imaging Program at Palomar Observatory. Publications of the Astronomical Society of the Pacific, 2011, 123, 74-86.	3.1	147
6	DISCOVERY OF A COMPANION CANDIDATE IN THE HD 169142 TRANSITION DISK AND THE POSSIBILITY OF MULTIPLE PLANET FORMATION. Astrophysical Journal Letters, 2014, 792, L23.	8.3	142
7	POLARIMETRY WITH THE GEMINI PLANET IMAGER: METHODS, PERFORMANCE AT FIRST LIGHT, AND THE CIRCUMSTELLAR RING AROUND HR 4796A. Astrophysical Journal, 2015, 799, 182.	4.5	139
8	RECONNAISSANCE OF THE HR 8799 EXOSOLAR SYSTEM. I. NEAR-INFRARED SPECTROSCOPY. Astrophysical Journal, 2013, 768, 24.	4.5	131
9	DETECTION AND CHARACTERIZATION OF EXOPLANETS USING PROJECTIONS ON KARHUNEN–LOEVE EIGENIMAGES: FORWARD MODELING. Astrophysical Journal, 2016, 824, 117.	4.5	126
10	ORBITAL MOTION OF HR 8799 b, c, d USING <i>HUBBLE SPACE TELESCOPE</i> DATA FROM 1998: CONSTRAINTS ON INCLINATION, ECCENTRICITY, AND STABILITY. Astrophysical Journal, 2011, 741, 55.	4.5	118
11	Characterizing 51 Eri b from 1 to 5Âμm: A Partly Cloudy Exoplanet. Astronomical Journal, 2017, 154, 10.	4.7	110
12	<i>î²</i> PICTORIS' INNER DISK IN POLARIZED LIGHT AND NEW ORBITAL PARAMETERS FOR <i>β</i> PICTORIS <i>b</i> . Astrophysical Journal, 2015, 811, 18.	4.5	108
13	Optimal dark hole generation via two deformable mirrors with stroke minimization. Applied Optics, 2009, 48, 6296.	2.1	106
14	RECONNAISSANCE OF THE HR 8799 EXOSOLAR SYSTEM. II. ASTROMETRY AND ORBITAL MOTION. Astrophysical Journal, 2015, 803, 31.	4.5	106
15	Chasing Shadows: Rotation of the Azimuthal Asymmetry in the TW Hya Disk*. Astrophysical Journal, 2017, 835, 205.	4.5	99
16	Complex Spiral Structure in the HD 100546 Transitional Disk as Revealed by GPI and MagAO. Astronomical Journal, 2017, 153, 264.	4.7	99
17	Orbits for the Impatient: A Bayesian Rejection-sampling Method for Quickly Fitting the Orbits of Long-period Exoplanets. Astronomical Journal, 2017, 153, 229.	4.7	98
18	Improving and Assessing Planet Sensitivity of the GPI Exoplanet Survey with a Forward Model Matched Filter. Astrophysical Journal, 2017, 842, 14.	4.5	96

#	Article	IF	CITATIONS
19	THE ORBIT AND TRANSIT PROSPECTS FOR Î ² PICTORIS b CONSTRAINED WITH ONE MILLIARCSECOND ASTROMETRY. Astronomical Journal, 2016, 152, 97.	4.7	95
20	Dynamical Constraints on the HR 8799 Planets with GPI. Astronomical Journal, 2018, 156, 192.	4.7	95
21	APODIZED PUPIL LYOT CORONAGRAPHS FOR ARBITRARY APERTURES. III. QUASI-ACHROMATIC SOLUTIONS. Astrophysical Journal, 2011, 729, 144.	4.5	93
22	1–2.4 μ4m Near-IR Spectrum of the Giant Planet β Pictoris b Obtained with the Gemini Planet Imager. Astronomical Journal, 2017, 153, 182.	4.7	92
23	HIGH-CONTRAST IMAGING WITH AN ARBITRARY APERTURE: ACTIVE COMPENSATION OF APERTURE DISCONTINUITIES. Astrophysical Journal, 2013, 769, 102.	4.5	87
24	APODIZED PUPIL LYOT CORONAGRAPHS FOR ARBITRARY APERTURES. V. HYBRID SHAPED PUPIL DESIGNS FOR IMAGING EARTH-LIKE PLANETS WITH FUTURE SPACE OBSERVATORIES. Astrophysical Journal, 2016, 818, 163.	4.5	87
25	APPLICATION OF A DAMPED LOCALLY OPTIMIZED COMBINATION OF IMAGES METHOD TO THE SPECTRAL CHARACTERIZATION OF FAINT COMPANIONS USING AN INTEGRAL FIELD SPECTROGRAPH. Astrophysical Journal, Supplement Series, 2012, 199, 6.	7.7	86
26	Non-negative Matrix Factorization: Robust Extraction of Extended Structures. Astrophysical Journal, 2018, 852, 104.	4.5	83
27	An Optical/Near-infrared Investigation of HD 100546 b with the Gemini Planet Imager and MagAO. Astronomical Journal, 2017, 153, 244.	4.7	81
28	GEMINI PLANET IMAGER SPECTROSCOPY OF THE HR 8799 PLANETS c AND d. Astrophysical Journal Letters, 2014, 794, L15.	8.3	80
29	THE κ ANDROMEDAE SYSTEM: NEW CONSTRAINTS ON THE COMPANION MASS, SYSTEM AGE, AND FURTHER MULTIPLICITY. Astrophysical Journal, 2013, 779, 153.	4.5	79
30	DIRECT IMAGING OF AN ASYMMETRIC DEBRIS DISK IN THE HD 106906 PLANETARY SYSTEM. Astrophysical Journal, 2015, 814, 32.	4.5	79
31	SPECTROSCOPIC CHARACTERIZATION OF HD 95086 b WITH THE GEMINI PLANET IMAGER. Astrophysical Journal, 2016, 824, 121.	4.5	78
32	ASTROMETRIC CONFIRMATION AND PRELIMINARY ORBITAL PARAMETERS OF THE YOUNG EXOPLANET 51 ERIDANI b WITH THE GEMINI PLANET IMAGER. Astrophysical Journal Letters, 2015, 814, L3.	8.3	77
33	Review of small-angle coronagraphic techniques in the wake of ground-based second-generation adaptive optics systems. Proceedings of SPIE, 2012, , .	0.8	71
34	Gemini Planet Imager observational calibrations I: Overview of the GPI data reduction pipeline. Proceedings of SPIE, 2014, , .	0.8	70
35	SPECKLE SUPPRESSION WITH THE PROJECT 1640 INTEGRAL FIELD SPECTROGRAPH. Astrophysical Journal, 2011, 729, 132.	4.5	68
36	FIRST IMAGES OF DEBRIS DISKS AROUND TWA 7, TWA 25, HD 35650, AND HD 377. Astrophysical Journal Letters, 2016, 817, L2.	8.3	64

#	Article	IF	CITATIONS
37	Debris Disk Results from the Gemini Planet Imager Exoplanet Survey's Polarimetric Imaging Campaign. Astronomical Journal, 2020, 160, 24.	4.7	64
38	THE FIRST <i>H</i> -BAND SPECTRUM OF THE GIANT PLANET β PICTORIS b. Astrophysical Journal Letters, 2015, 798, L3.	8.3	61
39	FIVE DEBRIS DISKS NEWLY REVEALED IN SCATTERED LIGHT FROM THE <i>HUBBLE SPACE TELESCOPE</i> NICMOS ARCHIVE. Astrophysical Journal Letters, 2014, 786, L23.	8.3	60
40	DISCOVERY OF A SUBSTELLAR COMPANION TO THE NEARBY DEBRIS DISK HOST HR 2562. Astrophysical Journal Letters, 2016, 829, L4.	8.3	60
41	FIRST SCATTERED-LIGHT IMAGE OF THE DEBRIS DISK AROUND HD 131835 WITH THE GEMINI PLANET IMAGER. Astrophysical Journal Letters, 2015, 815, L14.	8.3	54
42	Evidence That the Directly Imaged Planet HD 131399 Ab Is a Background Star. Astronomical Journal, 2017, 154, 218.	4.7	52
43	APODIZED PUPIL LYOT CORONAGRAPHS FOR ARBITRARY APERTURES. II. THEORETICAL PROPERTIES AND APPLICATION TO EXTREMELY LARGE TELESCOPES. Astrophysical Journal, 2009, 695, 695-706.	4.5	50
44	GPI Spectra of HR 8799 c, d, and e from 1.5 to 2.4 μm with KLIP Forward Modeling. Astronomical Journal, 2018, 155, 226.	4.7	50
45	APODIZED PUPIL LYOT CORONAGRAPHS FOR ARBITRARY APERTURES. IV. REDUCED INNER WORKING ANGLE AND INCREASED ROBUSTNESS TO LOW-ORDER ABERRATIONS. Astrophysical Journal, 2015, 799, 225.	4.5	43
46	Sensing Phase Aberrations behind Lyot Coronagraphs. Astrophysical Journal, 2008, 688, 701-708.	4.5	41
47	GEMINI PLANET IMAGER OBSERVATIONS OF THE AU MICROSCOPII DEBRIS DISK: ASYMMETRIES WITHIN ONE ARCSECOND. Astrophysical Journal Letters, 2015, 811, L19.	8.3	41
48	The SHARDDS survey: First resolved image of the HD 114082 debris disk in the Lower Centaurus Crux with SPHERE. Astronomy and Astrophysics, 2016, 596, L4.	5.1	36
49	First Scattered-light Images of the Gas-rich Debris Disk around 49 Ceti. Astrophysical Journal Letters, 2017, 834, L12.	8.3	36
50	An Exo–Kuiper Belt with an Extended Halo around HD 191089 in Scattered Light. Astrophysical Journal, 2019, 882, 64.	4.5	34
51	The Vector Vortex Coronagraph: sensitivity to central obscuration, low-order aberrations, chromaticism, and polarization. Proceedings of SPIE, 2010, , .	0.8	33
52	DESIGN OF PHASE INDUCED AMPLITUDE APODIZATION CORONAGRAPHS OVER SQUARE APERTURES. Astrophysical Journal, Supplement Series, 2011, 195, 25.	7.7	33
53	BRINGING "THE MOTH―TO LIGHT: A PLANET-SCULPTING SCENARIO FOR THE HD 61005 DEBRIS DISK. Astronomical Journal, 2016, 152, 85.	4.7	33
54	Archival legacy investigations of circumstellar environments: overview and first results. Proceedings of SPIE, 2014, , .	0.8	30

#	Article	IF	CITATIONS
55	The Gemini Planet Imager Exoplanet Survey: Dynamical Mass of the Exoplanet β Pictoris b from Combined Direct Imaging and Astrometry. Astronomical Journal, 2020, 159, 71.	4.7	29
56	Multiband GPI Imaging of the HR 4796A Debris Disk. Astrophysical Journal, 2020, 898, 55.	4.5	29
57	Polychromatic Compensation of Propagated Aberrations for Highâ€Contrast Imaging. Astrophysical Journal, 2007, 666, 609-625.	4.5	28
58	Direct Imaging of the HD 35841 Debris Disk: A Polarized Dust Ring from Gemini Planet Imager and an Outer Halo from HST/STIS. Astronomical Journal, 2018, 156, 47.	4.7	28
59	THE PECULIAR DEBRIS DISK OF HD 111520 AS RESOLVED BY THE GEMINI PLANET IMAGER. Astrophysical Journal, 2016, 826, 147.	4.5	27
60	Project 1640: the world's first ExAO coronagraphic hyperspectral imager for comparative planetary science. Proceedings of SPIE, 2012, , .	0.8	26
61	ESTABLISHING \hat{I}_{\pm} Oph AS A PROTOTYPE ROTATOR: IMPROVED ASTROMETRIC ORBIT. Astrophysical Journal, 2011, 726, 104.	4.5	25
62	DIRECT SPECTRUM OF THE BENCHMARK T DWARF HD 19467 B. Astrophysical Journal Letters, 2015, 798, L43.	8.3	25
63	KNOW THE STAR, KNOW THE PLANET. V. CHARACTERIZATION OF THE STELLAR COMPANION TO THE EXOPLANET HOST STAR HD 177830. Astronomical Journal, 2015, 150, 103.	4.7	24
64	Dynamical Evidence of a Spiral Arm–driving Planet in the MWC 758 Protoplanetary Disk. Astrophysical Journal Letters, 2020, 898, L38.	8.3	24
65	GPI Spectroscopy of the Mass, Age, and Metallicity Benchmark Brown Dwarf HD 4747 B. Astrophysical Journal, 2018, 853, 192.	4.5	23
66	Using Data Imputation for Signal Separation in High-contrast Imaging. Astrophysical Journal, 2020, 892, 74.	4.5	23
67	Direct imaging of sub-Jupiter mass exoplanets with <i>James Webb Space Telescope</i> coronagraphy. Monthly Notices of the Royal Astronomical Society, 2021, 501, 1999-2016.	4.4	23
68	THE PDS 66 CIRCUMSTELLAR DISK AS SEEN IN POLARIZED LIGHT WITH THE GEMINI PLANET IMAGER. Astrophysical Journal Letters, 2016, 818, L15.	8.3	22
69	Hubble Space Telescope Scattered-light Imaging and Modeling of the Edge-on Protoplanetary Disk ESO-Hα 569. Astrophysical Journal, 2017, 851, 56.	4.5	22
70	A Decade of MWC 758 Disk Images: Where Are the Spiral-arm-driving Planets?. Astrophysical Journal Letters, 2018, 857, L9.	8.3	22
71	Multiband Polarimetric Imaging of HR 4796A with the Gemini Planet Imager. Astronomical Journal, 2020, 160, 79.	4.7	22
72	ACCESS: a concept study for the direct imaging and spectroscopy of exoplanetary systems. Proceedings of SPIE, 2010, , .	0.8	21

#	Article	IF	CITATIONS
73	Finding the Needles in the Haystacks: High-fidelity Models of the Modern and Archean Solar System for Simulating Exoplanet Observations. Publications of the Astronomical Society of the Pacific, 2017, 129, 124401.	3.1	21
74	<i>S4</i> : A SPATIAL-SPECTRAL MODEL FOR SPECKLE SUPPRESSION. Astrophysical Journal, 2014, 794, 161.	4.5	20
75	AN IMAGE-PLANE ALGORITHM FOR <i>JWST </i> 'S NON-REDUNDANT APERTURE MASK DATA. Astrophysical Journal, 2015, 798, 68.	4.5	19
76	IMAGING AN 80 au RADIUS DUST RING AROUND THE F5V STAR HD 157587. Astronomical Journal, 2016, 152, 128.	4.7	19
77	The Gemini Planet Imager View of the HD 32297 Debris Disk. Astronomical Journal, 2020, 159, 251.	4.7	19
78	HIGH-RESOLUTION INFRARED IMAGING AND SPECTROSCOPY OF THE Z CANIS MAJORIS SYSTEM DURING QUIESCENCE AND OUTBURST. Astrophysical Journal Letters, 2013, 763, L9.	8.3	18
79	CHARACTERIZING THE ATMOSPHERES OF THE HR8799 PLANETS WITH <i>HST</i> /WFC3. Astrophysical Journal Letters, 2015, 809, L33.	8.3	18
80	Gemini Planet Imager coronagraph testbed results. Proceedings of SPIE, 2010, , .	0.8	17
81	CONSTRAINING MASS RATIO AND EXTINCTION IN THE FU ORIONIS BINARY SYSTEM WITH INFRARED INTEGRAL FIELD SPECTROSCOPY. Astrophysical Journal, 2012, 757, 57.	4.5	17
82	A Bayesian Framework for Exoplanet Direct Detection and Non-detection. Astronomical Journal, 2018, 156, 196.	4.7	17
83	Apodized vortex coronagraph designs for segmented aperture telescopes. Proceedings of SPIE, 2016, , .	0.8	17
84	The LUVOIR architecture ``A'' coronagraph instrument. , 2017, , .		17
85	An Updated Visual Orbit of the Directly Imaged Exoplanet 51 Eridani b and Prospects for a Dynamical Mass Measurement with Gaia. Astronomical Journal, 2020, 159, 1.	4.7	16
86	Spiral Arm Pattern Motion in the SAO 206462 Protoplanetary Disk. Astrophysical Journal Letters, 2021, 906, L9.	8.3	16
87	High-contrast imager for complex aperture telescopes (HiCAT): 1. testbed design. Proceedings of SPIE, 2013, , .	0.8	15
88	A Layered Debris Disk around M Star TWA 7 in Scattered Light. Astrophysical Journal, 2021, 914, 95.	4.5	15
89	Review of high-contrast imaging systems for current and future ground- and space-based telescopes I: coronagraph design methods and optical performance metrics. , 2018, , .		15
90	The Gemini planet imager: first light and commissioning. Proceedings of SPIE, 2014, , .	0.8	14

#	Article	IF	CITATIONS
91	Searching for Planets Orbiting <i>α</i> Cen A with the <i>James Webb Space Telescope</i> . Publications of the Astronomical Society of the Pacific, 2020, 132, 015002.	3.1	14
92	Active compensation of aperture discontinuities for WFIRST-AFTA: analytical and numerical comparison of propagation methods and preliminary results with a WFIRST-AFTA-like pupil. Journal of Astronomical Telescopes, Instruments, and Systems, 2015, 2, 011008.	1.8	12
93	Lyot coronagraph design study for large, segmented space telescope apertures. Proceedings of SPIE, 2016, , .	0.8	12
94	Updated optical modeling of JWST coronagraph performance contrast, stability, and strategies. , 2018, , .		12
95	First Resolved Scattered-light Images of Four Debris Disks in Scorpius-Centaurus with the Gemini Planet Imager. Astronomical Journal, 2020, 159, 31.	4.7	12
96	Improved Orbital Constraints and Hα Photometric Monitoring of the Directly Imaged Protoplanet Analog HD 142527 B. Astronomical Journal, 2022, 164, 29.	4.7	12
97	SPECTRAL TYPING OF LATE-TYPE STELLAR COMPANIONS TO YOUNG STARS FROM LOW-DISPERSION NEAR-INFRARED INTEGRAL FIELD UNIT DATA. Astronomical Journal, 2012, 144, 14.	4.7	11
98	Space-based Coronagraphic Imaging Polarimetry of the TW Hydrae Disk: Shedding New Light on Self-shadowing Effects. Astrophysical Journal, 2018, 860, 115.	4.5	11
99	HST Survey of the Orion Nebula Cluster in the H ₂ O 1.4 μm Absorption Band. I. A Census of Substellar and Planetary-mass Objects. Astrophysical Journal, 2020, 896, 79.	4.5	11
100	Kernel Phase and Coronagraphy with Automatic Differentiation. Astrophysical Journal, 2021, 907, 40.	4.5	11
101	Assessing the performance limits of internal coronagraphs through end-to-end modeling: a NASA TDEM study. Proceedings of SPIE, 2011, , .	0.8	10
102	Polynomial Apodizers for Centrally Obscured Vortex Coronagraphs. Astronomical Journal, 2017, 154, 240.	4.7	10
103	The Gemini Planet Imager coronagraph testbed. Proceedings of SPIE, 2009, , .	0.8	9
104	Data processing and algorithm development for the WFIRST-AFTA coronagraph: reduction of noise free simulated images, analysis and spectrum extraction with reference star differential imaging. Proceedings of SPIE, 2015, , .	0.8	9
105	Post-processing of the HST STIS coronagraphic observations. , 2017, , .		9
106	Propagation of aberrations through phase-induced amplitude apodization coronagraph. Journal of the Optical Society of America A: Optics and Image Science, and Vision, 2011, 28, 189.	1.5	8
107	Active correction of aperture discontinuities (ACAD) for space telescope pupils: a parametic analysis. Proceedings of SPIE, 2015, , .	0.8	8
108	High-contrast imager for complex aperture telescopes (HiCAT): 3. first lab results with wavefront control. Proceedings of SPIE, 2015, , .	0.8	8

#	Article	IF	CITATIONS
109	Archival Legacy Investigations of Circumstellar Environments (ALICE): Statistical assessment of point source detections. Proceedings of SPIE, 2015, , .	0.8	8
110	Imaging the 44 au Kuiper Belt Analog Debris Ring around HD 141569A with GPI Polarimetry. Astronomical Journal, 2020, 159, 53.	4.7	8
111	Upgrading the Gemini planet imager: GPI 2.0. , 2018, , .		8
112	High-contrast imager for complex aperture telescopes (HiCAT): 5. first results with segmented-aperture coronagraph and wavefront control. , 2018, , .		8
113	Apodized pupil Lyot coronagraphs designs for future segmented space telescopes. , 2018, , .		8
114	The Gemini Planet Imager calibration testbed. Proceedings of SPIE, 2009, , .	0.8	7
115	On advanced estimation techniques for exoplanet detection and characterization using ground-based coronagraphs. Proceedings of SPIE, 2012, 8447, .	0.8	7
116	The LUVOIR Extreme Coronagraph for Living Planetary Systems (ECLIPS) II. Performance evaluation, aberration sensitivity analysis and exoplanet detection simulations. , 2019, , .		7
117	On the effects of pointing jitter, actuator drift, telescope rolls, and broadband detectors in dark hole maintenance and electric field order reduction. Journal of Astronomical Telescopes, Instruments, and Systems, 2020, 6, 1.	1.8	7
118	Practical numerical propagation of arbitrary wavefronts through PIAA optics. , 2010, , .		6
119	High-contrast Imager for Complex Aperture Telescopes (HICAT): II. Design overview and first light results. Proceedings of SPIE, 2014, , .	0.8	6
120	HST Survey of the Orion Nebula Cluster in the H ₂ O 1.4 μm Absorption Band. III. The Population of Substellar Binary Companions. Astrophysical Journal, 2020, 896, 81.	4.5	6
121	Wavefront error tolerancing for direct imaging of exo-Earths with a large segmented telescope in space. , 2019, , .		6
122	Direct Imaging as a Detection Technique for Exoplanets. , 2018, , 705-765.		5
123	Detection of a Low-mass Stellar Companion to the Accelerating A2IV Star HR 1645. Astronomical Journal, 2019, 158, 226.	4.7	5
124	Data processing and algorithm development for the WFIRST coronagraph: comparison of RDI and ADI strategies and impact of spatial sampling on post-processing. Proceedings of SPIE, 2016, , .	0.8	5
125	Sensitivity analysis for high-contrast missions with segmented telescopes. , 2017, , .		5
126	High contrast imaging with an arbitrary aperture: active correction of aperture discontinuities: fundamental limits and practical trade- offs. Proceedings of SPIE, 2014, , .	0.8	4

#	Article	IF	CITATIONS
127	Small-grid dithering strategy for improved coronagraphic performance with JWST. Proceedings of SPIE, 2014, , .	0.8	4
128	A Deep Search for Planets in the Inner 15 au around Vega. Astronomical Journal, 2018, 156, 214.	4.7	4
129	Sensitivity analysis for high-contrast imaging with segmented space telescopes. , 2018, , .		4
130	Pushing the Limits of Exoplanet Discovery via Direct Imaging with Deep Learning. Lecture Notes in Computer Science, 2020, , 322-338.	1.3	4
131	Advanced static speckle calibration for exoplanet imaging. , 2010, , .		3
132	High-contrast imager for Complex Aperture Telescopes (HiCAT). 4. Status and wavefront control development. Proceedings of SPIE, 2016, , .	0.8	3
133	Performance of the Gemini Planet Imager Non-redundant Mask and Spectroscopy of Two Close-separation Binaries: HR 2690 and HD 142527. Astronomical Journal, 2019, 157, 249.	4.7	3
134	Simulating JWST high contrast observations with PanCAKE. , 2021, , .		3
135	Flat field errors and intra-pixel sensitivities for non-redundant aperture masking interferometry on JWST NIRISS. , 2013, , .		3
136	Fundamental limits to high-contrast wavefront control. , 2017, , .		3
137	Optimal deformable mirror and pupil apodization combinations for apodized pupil Lyot coronagraphs with obstructed pupils. , 2018, , .		3
138	Apodized Pupil Lyot coronagraphs with arbitrary aperture telescopes: novel designs using hybrid focal plane masks. , 2018, , .		3
139	Making good use of JWST's coronagraphs: tools and strategies from a user's perspective. , 2018, , .		3
140	Aperture mask interferometry with an integral field spectrograph. Proceedings of SPIE, 2012, , .	0.8	2
141	A format standard for efficient interchange of high-contrast direct imaging science products. Proceedings of SPIE, 2014, , .	0.8	2
142	Wavefront control with algorithmic differentiation on the HiCAT testbed. , 2021, , .		2
143	Optimization of pyKLIP's forward model matched filter for the GPI Exoplanet Survey. , 2017, , .		2
144	Polynomial apodized vortex coronagraphs for obscured telescope pupils. , 2017, , .		2

#	Article	IF	CITATIONS
145	Capabilities of ACAD-OSM, an active method for the correction of aperture discontinuities. , 2017, , .		2
146	Wavelength calibration and closure phases with the Gemini Planet Imager IFS using its non-redundant mask. , 2013, , .		1
147	Analyzing the first JWST-NIRISS NRM test data. Proceedings of SPIE, 2014, , .	0.8	1
148	Optimal apodizations for on-axis vector vortex coronagraphs. Proceedings of SPIE, 2014, , .	0.8	1
149	Demonstration of vortex coronagraph concepts for on-axis telescopes on the Palomar Stellar Double Coronagraph. Proceedings of SPIE, 2014, , .	0.8	1
150	Three possible types of coronagraphs for the E-ELT PCS instrument. , 2014, , .		1
151	WFIRST-AFTA coronagraph performance: feedback from post-processing studies to overall design. , 2015, , .		1
152	Laser guide star spot shrinkage for affordable wavefront sensors. , 2016, , .		1
153	Direct Imaging as a Detection Technique for Exoplanets. , 2018, , 1-61.		1
154	HD 165054: An Astrometric Calibration Field for High-contrast Imagers in Baade's Window. Astronomical Journal, 2020, 159, 244.	4.7	1
155	Archival Legacy Investigation of Circumstellar Environments using KLIP algorithm on HST NICMOS coronagraphic data. Proceedings of the International Astronomical Union, 2013, 8, 30-31.	0.0	Ο
156	Newly Seen Debris Disks from the HST NICMOS Archive. Proceedings of the International Astronomical Union, 2013, 8, 354-355.	0.0	0
157	Apodized Pupil Lyot Coronagraphs: development of designs with reduced IWA and robustness to low-order aberrations. Proceedings of SPIE, 2014, , .	0.8	0
158	Correcting for the effects of pupil discontinuities with the ACAD method. , 2016, , .		0
159	Broadband Correction for High Contrast Imaging using Two Deformable Mirrors in Series. , 2009, , .		0